Chemistry Letters

http://www.csj.jp/journals/chem-lett/

Vol.33 No.7
July, 2004

CMLTAG
ISSN 0366-7022

Highlight Review

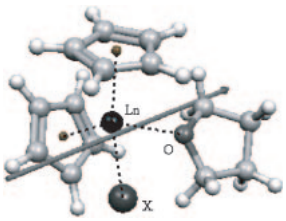

The optimized geometry structure of $Cp_2LnX(THF)$ (Cp = cyclopentadienyl, THF = tetrahydrofuran, Ln = La–Lu and X = halides. Unmarked white and gray balls represent hydrogen and carbon, respectively. The arrow indicates the direction of dipole moment.) In this article, the very recent theoretical calculations on organo-f-element complex are outlined.

The use of lanthanide complexes as catalysts in organic synthesis is currently of intense interest. In particular, organo-lanthanide complexes are of rapidly growing importance, and hence the understanding of the binding behavior of f orbital as well as the ionic/covalent characteristics of lanthanocene-based complexes is of significance with respect to their reactivity and their role as catalyst in organic synthesis. The purpose of this review is to give a survey of recent progress in theoretical studies on organo-f-element complexes and to highlight successful applications of density functional and quantum chemical molecular dynamics methods.

Letter

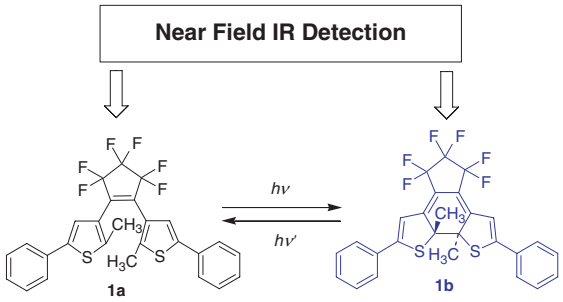

788 **Construction of Organic Monolayers with Electron Transfer Function on a Hydrogen Terminated Si(111) Surface via Silicon–Carbon Bond and Their Electrochemical Characteristics in Dark and Under Illumination**

Takuya Masuda and Kohei Uosaki

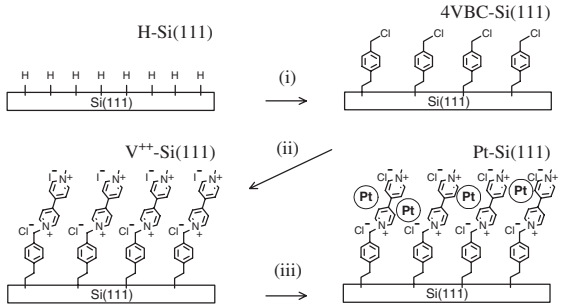

790 **Synthesis and Adsorption Property of Calixarene-*p*-sulfonate-intercalated Layered Double Hydroxides**

Satoru Sasaki, Sumio Aisawa, Hidetoshi Hirahara, Akira Sasaki, and Eiichi Narita

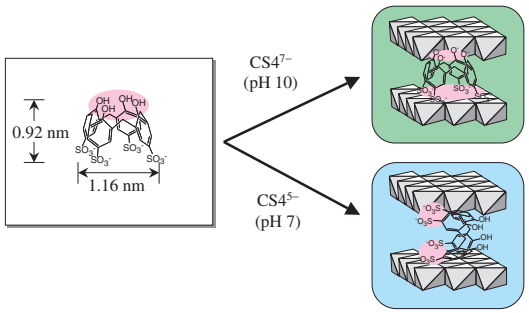

792 **Effect of Additives on Electrochemical Reduction of Oxygen in the Presence of Methanol**

Hidenobu Shiroishi, Yusuke Ayato, Keiji Kunimatsu, and Tatsuhiro Okada

Organic ligands or metal complexes which have pyridyl structures suppress methanol oxidation but not the oxygen reduction on platinum in sulfuric acid – methanol aqueous solution.

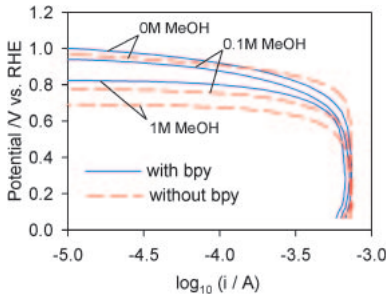

794 **Complementary Multicomplexation of Desymmetrized 2,2′-Bipyridine Ligands on Square Planar Pd(II) Centers**

Masahide Tominaga, Takahiro Kusukawa, Shigeru Sakamoto, Kentaro Yamaguchi, and Makoto Fujita

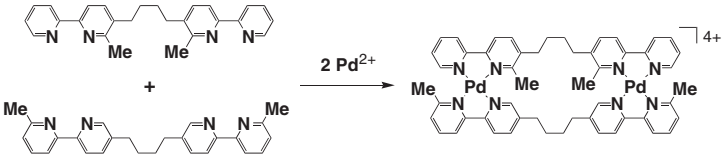

796 **Guaiacol Oxidation Products in the Enzyme-Activity Assay Reaction by Horseradish Peroxidase Catalysis**

Hiroyuki Tonami, Hiroshi Uyama, Ritsuko Nagahata, and Shiro Kobayashi

Products of guaiacol oxidation by HRP

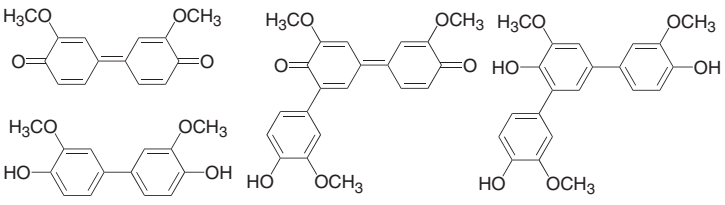

798 **Pressure-dependent Activity of Dihydrofolate Reductase from a Deep-sea Bacterium *Shewanella violacea* Strain DSS12**

Eiji Ohmae, Kazumasa Kubota, Kaoru Nakasone, Chiaki Kato, and Kunihiko Gekko

The enzyme activity of svDHFR increases with pressure, to at most 30% at 100 MPa, in contrast with ecDHFR. It can be expected that svDHFR has distinguished characteristics in enzyme kinetics and structural fluctuation to adapt itself to deep-sea conditions.

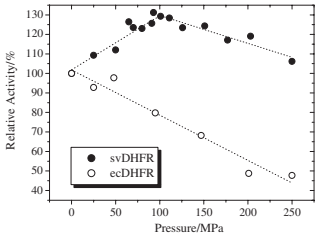

800 **Drastic Enhancement of SCR of NO over Ir Catalyst through Formation of Metallic Iridium on Na-zeolite**

Junji Shibata, Hisao Yoshida, Atsushi Satsuma, and Tadashi Hattori

Use of Na-zeolite as a support for Ir catalyst leads to preference formation of metallic iridium, on which the selective NO reduction effectively proceeds in the co-existence of CO and H_2.

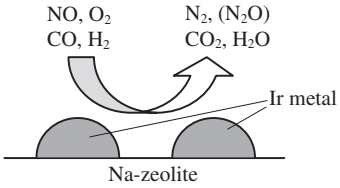

802 **Supercritical Microemulsions as Nanoreactors for Manufacturing ZnS Nanophosphors**

Te-Wen Kuo, Chien-Yueh Tung, Yung-Chan Lin, and Shyue-Ming Jang

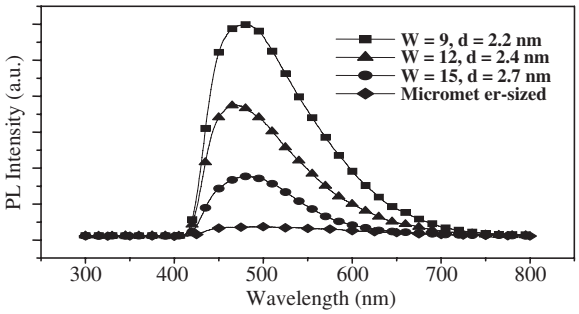

804 **One-step Route to Single-crystal γ-Mn_3O_4 Nanorods in Alcohol–Water System**

Baojun Yang, Hanmei Hu, Cun Li, Xiaogang Yang, Qiaowei Li, and Yitai Qian

A one-step low-temperature alcohol–water thermal route has been developed to synthesize single-crystal γ-Mn_3O_4 nanorods with diameters of 50–120 nm, and lengths of up to several tens micrometers.

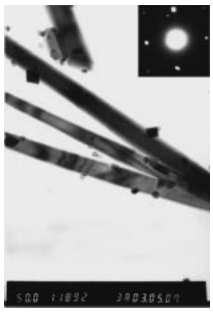

806 **Novel Surface-modified Molecularly Imprinted Polymer Focused on the Removal of Interference in Environmental Water Samples**

Yoshiyuki Watabe, Ken Hosoya, Nobuo Tanaka, Takuya Kubo, Takuya Kondo, and Masatosi Morita

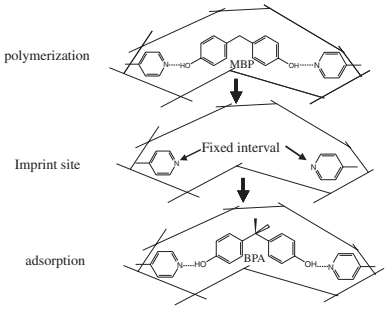

808 **Nitration of Aromatic Compounds with Nitric Acid Catalyzed by Ionic Liquids**

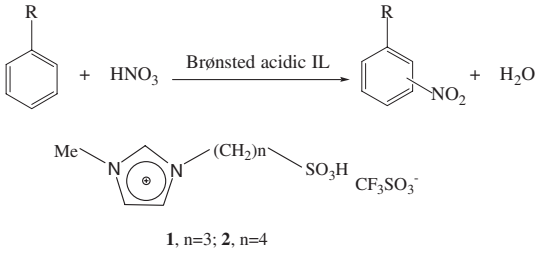

1, n=3; **2**, n=4

Kun Qiao and Chiaki Yokoyama

810 **Spontaneous Assembly Formation of Cyclic Dimer of β-Amino Acid in Water**

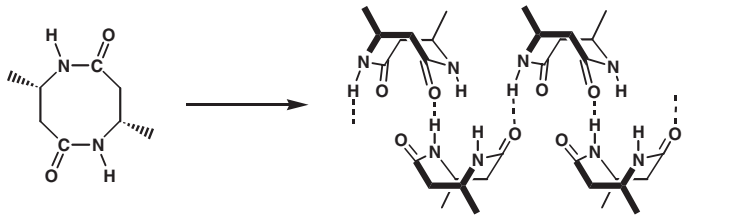

cyclic peptide assembly via hydrogen bonding

Futoshi Fujimura, Makoto Fukuda, Junji Sugiyama, Tomoyuki Morita, and Shunsaku Kimura

812 **Arrangement of Ferritin Molecules on a Gold Disk Array Fabricated on Highly Ordered Anodic Porous Alumina Substrate**

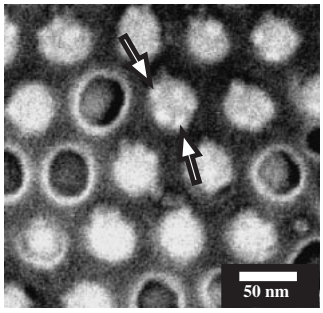

An array of ferritin molecules organized on Au nanodisks

Hideki Masuda, Hiromi Hogi, Kazuyuki Nishio, and Futoshi Matsumoto

814 **Useful Synthesis of Fragment A–C–D of a Thiostrepton-type Macrocyclic Antibiotic, Thiocilline I**

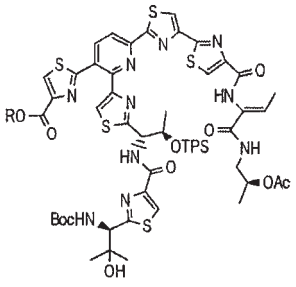

Shuusuke Suzuki, Yasuchika Yonezawa, and Chung-gi Shin

816 **Effect of Paramagnetic Fe^{3+} on T_1^H in PVA/montmorillonite-clay Nanocomposites**

We examined the effect of the paramagnetic Fe^{3+} ions on the ^1H spin-lattice relaxation time (T_1^H) for PVA/montmorillonite-clay nanocomposites indirectly observed from the conventional ^{13}C CPMAS NMR. Rapid decrease of the T_1^H values with the amount of montmorillonite clay was observed for the nanocomposites, while for a PVA/saponite nanocomposite including no Fe^{3+} ions such a decrease was not detected. This decrease relates on both amount of the paramagnetic Fe^{3+} ions and dispersion of clay in nanocomposites. By analyzing the effect of Fe^{3+} ions on T_1^H quantitatively, we found that the dispersion and amount of iron for clay are detectable in a nanocomposite nondestructively.

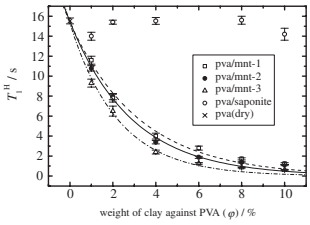

Atsushi Asano, Miho Shimizu, and Takuzo Kurotsu

818 **Hydrothermal Synthesis of Layered $Li[Ni_{0.5}Mn_{0.5}]O_2$ as Lithium Intercalation Material**

Seung-Taek Myung, Myung-Hoon Lee, Sang-Ho Park, and Yang-Kook Sun

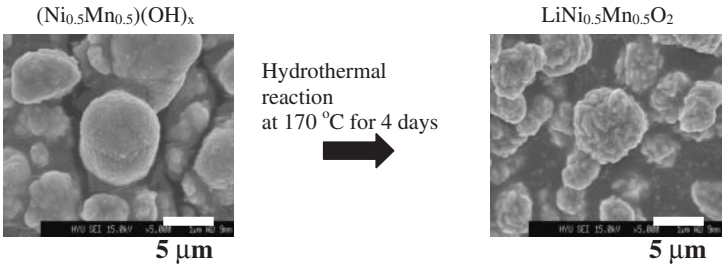

820 **Dissolution of Phthalocyanines in Dense Carbon Dioxide and Its Solvatochromic Behavior under Pressureized Conditions**

Hajime Kawanami, Yutaka Ikushima, and Nagao Kobayashi

Soluble phthalocyanines and subphthalocyanine into $scCO_2$ were found for the first time, and these compounds can be used as indicators to measure the solvent polarity in supercritical CO_2 conditions.

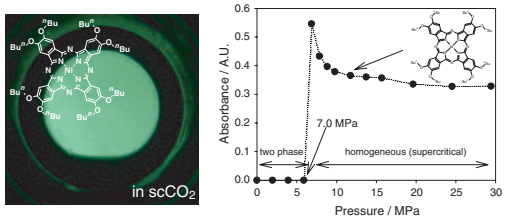

822 **A New Route to Control Product Selectivity in the Oxidative Dehydrogenation of Cyclohexane and Cyclohexene**

Yujun Zhu, Jing Li, Xiangguang Yang, and Yue Wu

High selectivity (almost 100%) to cyclohexene, 1,3-cyclohexadiene can be obtained by using the above approach in gas phase partial oxidation of cyclohexane, cyclohexene, respectively.

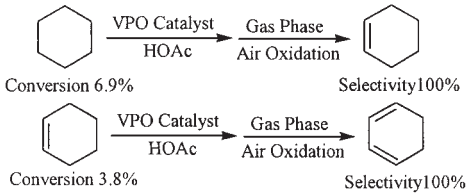

824 **Evaluation of the Relationship between the Catalyst Structure and Regio- as well as Stereoselectivity in the Chiral Ammonium Bifluoride–Catalyzed Asymmetric Addition of Silyl Nitronates to α,β-Unsaturated Aldehydes**

Takashi Ooi, Kumiko Morimoto, Kanae Doda, and Keiji Maruoka

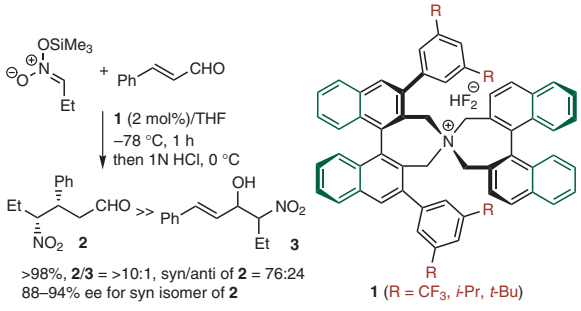

826 **Cobalt Ferrite Nanoparticles Prepared by Coprecipitation/Mechanochemical Treatment**

Huaming Yang, Xiangchao Zhang, Aidong Tang, and Guanzhou Qiu

Calcination can promote the crystallization of $CoFe_2O_4$ nanoparticles. The crystal grows primarily by means of an interfacial reaction during annealing.

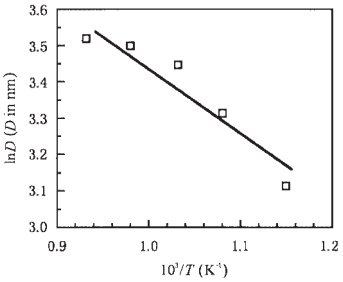

828 **Periodic Pulse Electrodeposition to Synthesize Ultra-high Density CdS Nanowire Arrays Templated by SBA-15 Mesoporous Films**

Jinlou Gu, Jianlin Shi, Hangrong Chen, Liangming Xiong, Weihua Shen, and Meilin Ruan

The high-density CdS nanowire arrays, which are the negative replica of the parent SBA-15 mesoporous thin films with a stoichiometric composition, have been synthesized through a newly developed periodic pulse electrodeposition route.

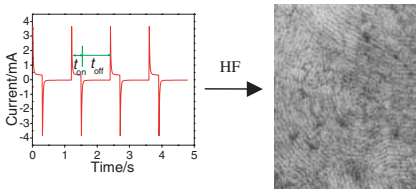

830 **Synthesis and Optical Properties of Novel Nickel Disulfide Dendritic Nanostructures**

Rui Luo, Xia Sun, Lifeng Yan, and Wenming Chen

Dendritic NiS_2 nanostructures are synthesized via the reaction between $NiCl_2 \cdot 6H_2O$ and CS_2 in poly (MMA-*co*-EA) gel using γ irradiation.

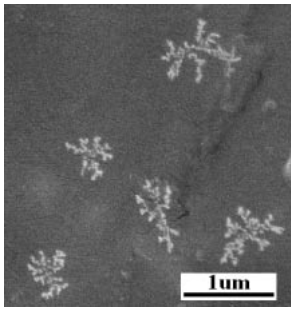

832 **Cobalt-Catalyzed Allylic Substitution Reaction of Allylic Ethers with Phenyl and Trimethylsilylmethyl Grignard Reagents**

Keiya Mizutani, Hideki Yorimitsu, and Koichiro Oshima

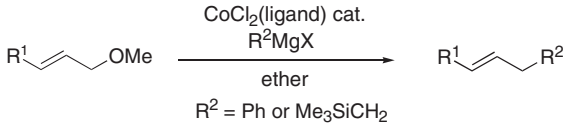

834 **Facile Oxidation of Aldehydes to Esters Using S·SnO_2/SBA-1–H_2O_2**

Guang Qian, Rui Zhao, Dong Ji, Gaomeng Lu, Yanxing Qi, and Jishuan Suo

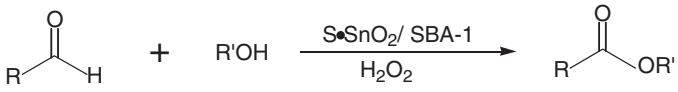

836 **A Facile Synthesis of CdSe and CdTe Nanorods Assisted by Myristic Acid**

Wei Nie, Lijia An, Bingzheng Jiang, and Xiang-Ling Ji

A simple, productive, low-cost route was developed to synthesize the high-quality 1-D nanorods of CdE (E = Se, Te) with different aspect ratio using myristic acid (MA) as a complexing agent. The reaction is performed under mild conditions and relatively low temperatures. It facilitates a large-scale production in future.

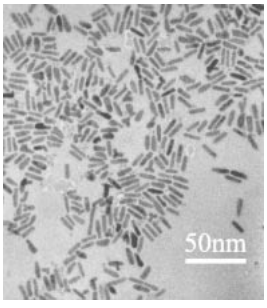

838 **Synthesis of Artificial Opals with Uniform Mesoporous Silica Spheres**

Chau-Nan Chen, Hong-Ping Lin, Chih-Pin Tsai, and Chin-Yuan Tang

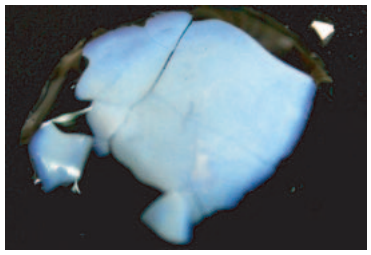

A light-blue artificial opal obtained with the highly uniform mesoporous silica spheres.

840 **Preparation of Water-soluble PEGylated Semiconductor Nanocrystals**

Eui-Chul Kang, Atsuhiko Ogura, Kazunori Kataoka, and Yukio Nagasaki

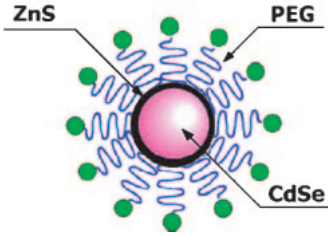

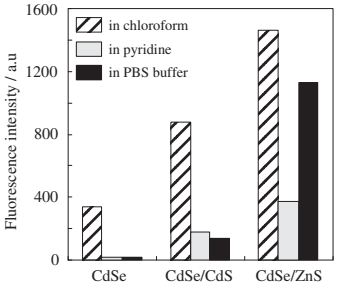

842 **Template-Directed Electrodeposition of Lamellar Platinum Nanostructures**

Ji K. Zhao, Xiao Chen, Li Y. Jiao, Yong C. Chai, Guo D. Zhang, and Jie Liu

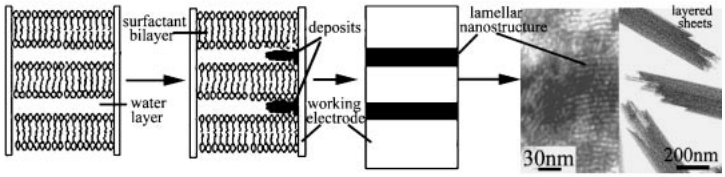

844 **Reversible Optical Rotation Change According to the Enantiospecific Photochromic Reaction of [2.2]Metacyclophan-1-ene**

Michinori Takeshita and Takehiko Yamato

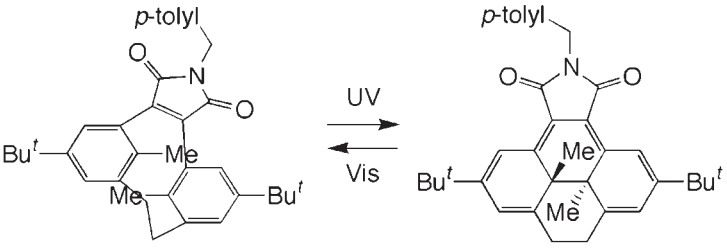

846 **Preparation of Deuterium Labelled Organophosphonium Salts (Wittig Salts) under Hydrothermal Condition Catalyzed by Molecular Sieves**

Mitsuru Yamamoto, Koichiro Oshima, and Seijiro Matsubara

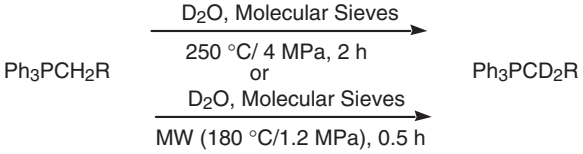

848 **Novel Photochromic Behavior of Benzoylhemithioindigo Based on Photodimerization**

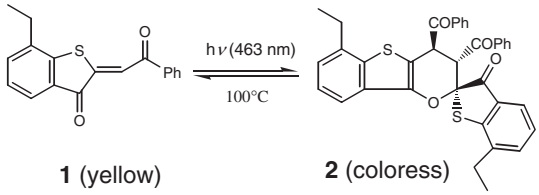

Kiyoshi Tanaka, Kazuto Taguchi, Satoru Iwata, and Takayuki Irie

Irradiation of **1** produces the [2+4] type of cycloadduct **2**, which is dissociated back to **1** on heating. The reversible photochromic property of **1** is described.

850 **Fluoride-selective Colorimetric Sensors Based on Hydrazone Functionality**

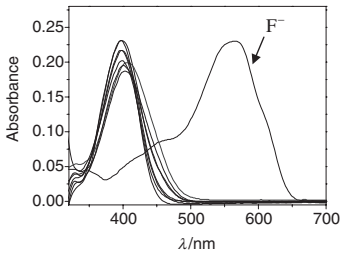

The changes of the UV–vis absorption spectra of compound **2** (1×10^{-5} mol/L) upon addition of 100 equiv. of anions (F^-, $H_2PO_4^-$, Cl^-, AcO^-, HSO_4^-, Br^-, NO_3^-, ClO_4^-, and I^-) in acetonitrile, respectively.

Lili Zhou, Xiaohong Zhang, and Shikang Wu

852 **Formation of Hollow Submicrometer Spheres of Nickel Selenides**

Hollow submicrometer spheres of nickel selenides $Ni_{0.85}Se$ and $NiSe_2$ have been successfully prepared in one step via hydrothermal reduction route under mild conditions employing sodium dodecyl sulfate as a surfactant. The composition of nickel selenides can be easily controlled by adjusting the molar ratios of reactants. The synthetic strategy can provide an effective and general route to the formation of other hollow spheres.

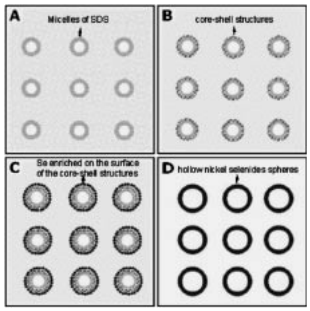

Xiaohe Liu, Guanzhou Qiu, Junwei Wang, and Yadong Li

854 **Radical Carbonylation of 1,5-Enynes Using TTMSS as a Chain Carrier. Unexpected Formation of Persistent 3-Silyl-1-siloxyallyl Radicals Serving as a Chain Breaking Path**

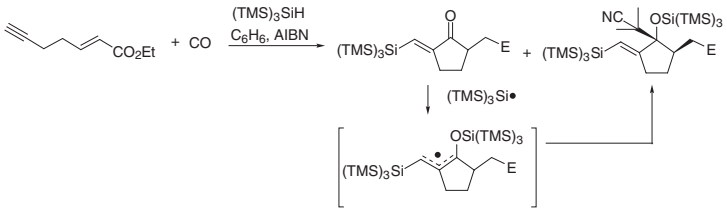

Takahide Fukuyama, Yoshitaka Uenoyama, Shinya Oguri, Noboru Otsuka, and Ilhyong Ryu

856 **Self-assembly of Guanidinium Hexagonal Carboxylate: How Many H-bonds and H-bonding Pattern between $ArCOO^-$ and $C(NH_2)_3^+$?**

In guanidinium hexacarboxylate, $\mathbf{H}\cdot G_6\cdot 2H_2O$ (**2**, G = $C(NH_2)_3$, the guanidinium cations and the side pyridinecarboxylate rings are self-assembled via multiple H-bonds (up to 6 H-bonds for each pyridinecarboxylate ring) into zigzag-like ribbons which located between the hexahost **H** core plane layers. The H-bonds garph set present in the zigzag ribbons are $R_2^2(8)$ [α], $R_2^1(6)$ [β], $R_2^2(10)$ [γ], $R_1^2(6)$ [δ], $R_2^3(12)$ [Ж], $R_5^3(10)$ [Ω], $R_8^6(24)$ [Ψ] and $R_8^4(24)$ [Φ].

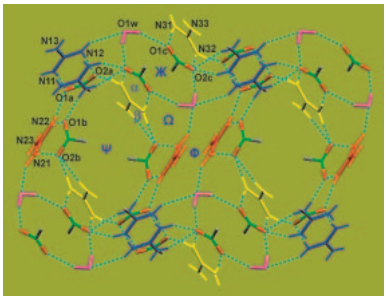

Chi Yang and Wing-Tak Wong

858 **Copolymerization of Aziridines and Carbon Monoxide Catalyzed by a Heterodinuclear Organopalladinum–Cobalt Complex**

Nobuyuki Komine, Shin-ichi Tanaka, Susumu Tsutsuminai, Yoshifumi Akahane, Masafumi Hirano, and Sanshiro Komiya

Heterodinuclear organopalladium-cobalt complex having a 2,2'-bipyridine ligand (bpy)AcPd–$Co(CO)_4$ catalyzes copolymeriztion of unsubstituted and both *C*- and *N*-monosubstituted aziridines, such as aziridine, 2-methylaziridine, and *N*-ethylaziridine, and CO (3–6 MPa) in THF at 100 °C for 6 h.

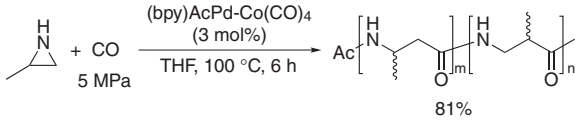

860 **Templated Assembly of a Monolayer Consisting of a Coordination Nanobox at Air–Water Interface**

Masaru Aoyagi, Hiroyuki Minamikawa, and Toshimi Shimizu

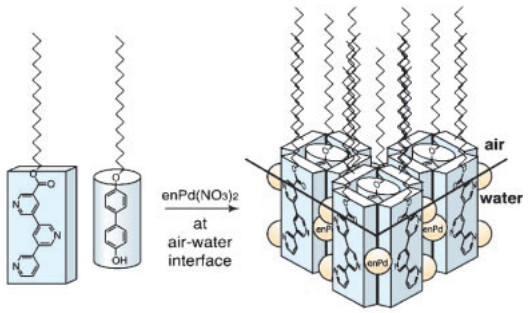

862 **Solvatochromic Shift of Phthalocyanine Q-band Governed by a Single Solvent Parameter**

Hiroaki Isago, Yutaka Kagaya, and Akiyuki Matsushita

Solvatochromic shift of Q-band for some octahedral phthalocyanine complexes is governed only by refractive index of the solvent, indicating that interaction of phthalocyanine transition dipole moment and induced dipole moment generated in the surrounding solvent molecules is predominant.

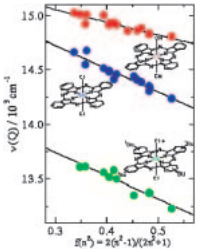

864 **S_N2 Type Hydrolysis of Secondary Alkyl Halides and Sulfonates in Hydrothermal Water**

Yuki Yamasaki, Takaharu Hirayama, Koichiro Oshima, and Seijiro Matsubara

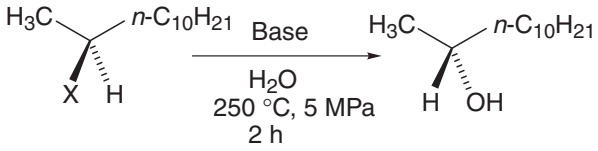

866 **Soluble Polymer-supported Synthesis of *trans* β-Lactams with High Diastereoselectivity**

Shan-Zhong Jian and Yan-Guang Wang

High diastereoselective synthesis of *trans* β-lactams on PEG was accomplished by introducing an auxiliary.

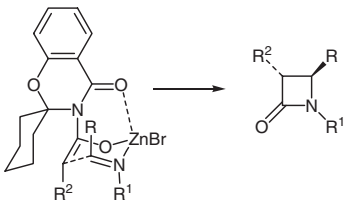

878 **_P_-Chiral Phosphinoselenoic Chlorides and Optically Active _P_-Chiral Phosphinoselenoic Amides: Synthesis and Stereospecific Interconversion with Extrusion and Addition Reactions of the Selenium Atom**

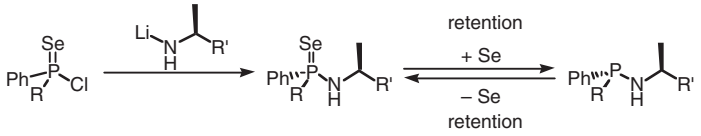

Tsutomu Kimura and Toshiaki Murai

880 **Single-crystalline $PbCrO_4$ Nanowires and Their Hydrothermal Transformation to Amorphous $PbCr_3O_{10}$ Nanotubes**

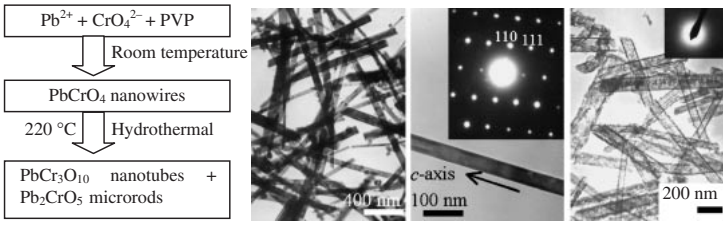

Xian-Luo Hu and Ying-Jie Zhu

882 **A Novel and Efficient Method for the Synthesis of α-Azidoketones and α-Ketothiocyanates**

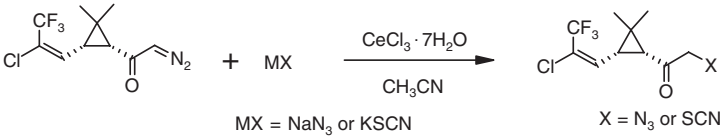

J. S. Yadav, B. V. Subba Reddy, and M. Srinivas

884 **Preparation of Lithium Hexafluorophosphate from LiF and P in Fluorine Atmosphere**

Lattice parameters of $LiPF_6$ prepared by L-AHF and F_2 direct methods

Method	L-AHF	F_2 direct
Space group	$R\bar{3}$ (no.148)	$R\bar{3}$ (no.148)
Cell parameter		
a_0(nm)	0.4933(1)	0.4932(2)
c_0(nm)	1.2657(2)	1.2641(5)
Z	3	3
Cell volume ($\times 10^{-28} m^3$)	2.668(1)	2.663(2)
Density ($\times 10^3 kg\ m^{-3}$)	2.836	2.841
Bond length (nm)		
F (18*f*) - P (3*b*)	0.161(4) 6×	0.160(3) 6×

Jae-Ho Kim, Kazushi Nagahara, Susumu Yonezawa, and Masayuki Takashima

886 **A New Class of Hydrophobic Ionic Liquids: Trialkyl(2-methoxyethyl)ammonium Perfluoroethyltrifluoroborate**

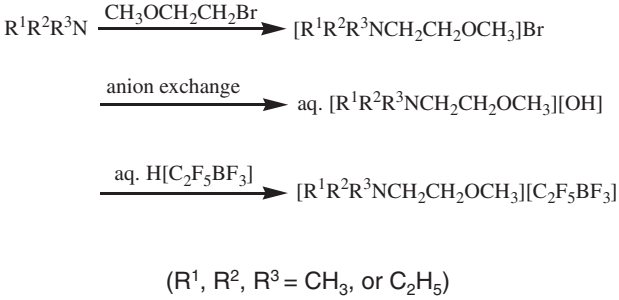

Zhi-Bin Zhou, Hajime Matsumoto, and Kuniaki Tatsumi

888 **Solid Phase Synthesis of Hydroxy Benzothiazepinones through Cyclative Release under Thermolysis**

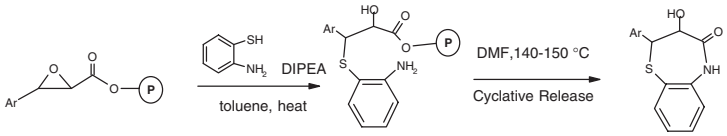

H. M. Sampath Kumar, P. Pawan Chakravarthy, M. Shesha Rao, Sipak Joyasawal, and J. S. Yadav

890 **Complex Formation and Gelation between Copolymers Containing Pendant Azobenzene Groups and Cyclodextrin Polymers**

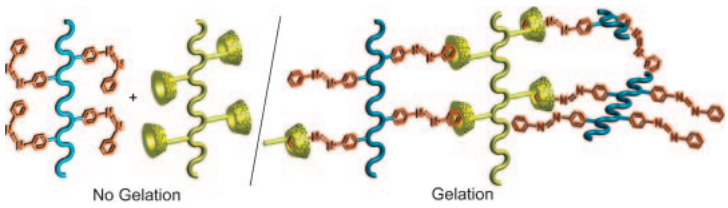

Yoshinori Takashima, Tomofumi Nakayama, Masahiko Miyauchi, Yoshinori Kawaguchi, Hiroyasu Yamaguchi, and Akira Harada

892 **Synthesis of Novel Spiro-condensed Dithienosiloles and the Application to Organic FET**

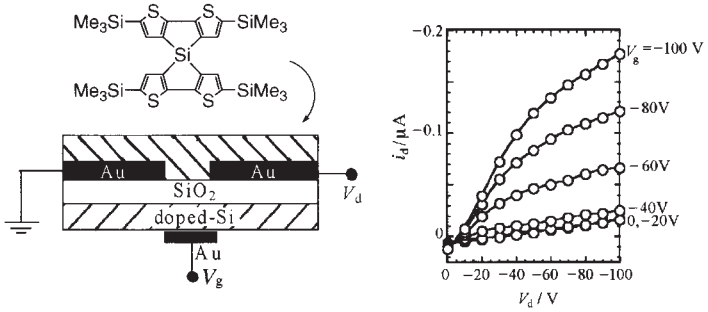

Joji Ohshita, Kwang-Hoi Lee, Daisuke Hamamoto, Yoshihito Kunugi, Junnai Ikadai, Young-Woo Kwak, and Atsutaka Kunai

894 **Nanotube Formation in Solution between β-Cyclodextrin and Cinchonine**

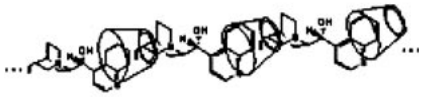

Xianhong Wen, Ming Guo, Ziyang Liu, and Fei Tan

896 **A Novel Ferromagnetically Coupled Dinuclear Manganese(II) Complex with Phenoxo Bridges**

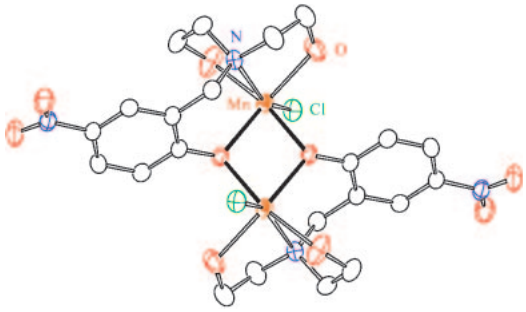

Satoshi Koizumi, Masayuki Nihei, and Hiroki Oshio

898 **Preparation of Cu_2S Nanoribbons from Cu(thiocarbamide)Cl·1/2H_2O Complex Nanowires by Solid-state Reaction at Room Temperature without Surfactants**

Chunnian Chen, Chunling Zhu, Linyun Hao, Yuan Hu, and Zuyao Chen

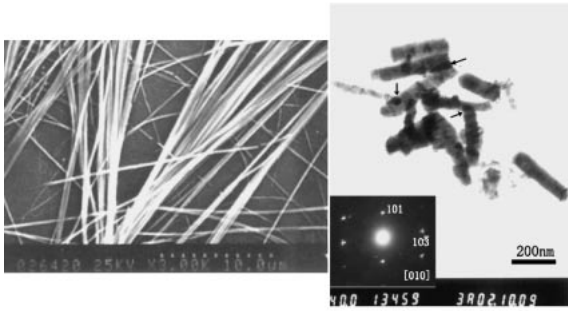

900 **Solvothermal Synthesis of Sodium and Potassium Tantalate Perovskite Nanocubes**

A low-temperature solution-based synthetic method was developed for the synthesis of nanocubic structures of sodium and potassium tantalates with the edge length of about 5 and 16 nm, respectively, without introducing any templates or catalysts.

Yu He and Yongfa Zhu

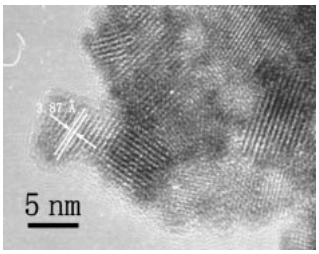

902 **Separation and Study of the Optical Properties of Silver Nanocubes by Capillary Electrophoresis**

Fu-Ken Liu and Fu-Hsiang Ko

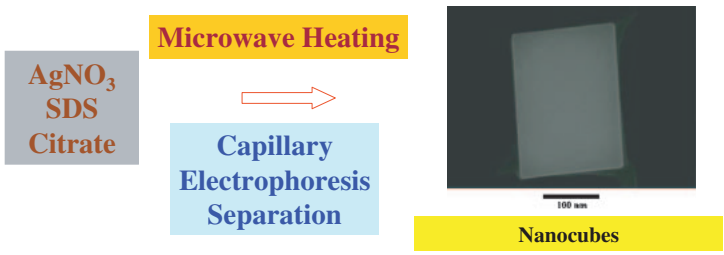

Described is a potential CE method to be used for the separation of differently shaped silver nanoparticles.

904 **Photochromism of Furylfulgide in a Single-crystalline Phase**

Seiya Kobatake and Masahiro Irie

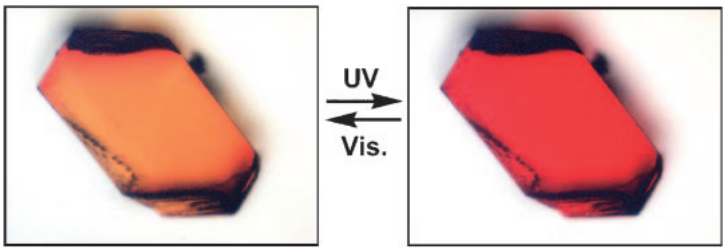

906 **Synthesis and Characterization of μ-Oxo-diiron(III) Complexes of Porphycenes with Electron-withdrawing Substituents**

Tatsushi Baba, Hisashi Shimakoshi, Isao Aritome, and Yoshio Hisaeda

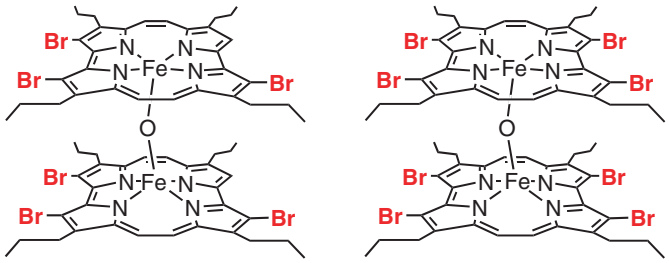

908 **Cu–Pd Bimetallic Cluster/AC as a Novel Catalyst for the Reduction of Nitrate to Nitrite**

Yoshinori Sakamoto, Kou Nakata, Yuichi Kamiya, and Toshio Okuhara

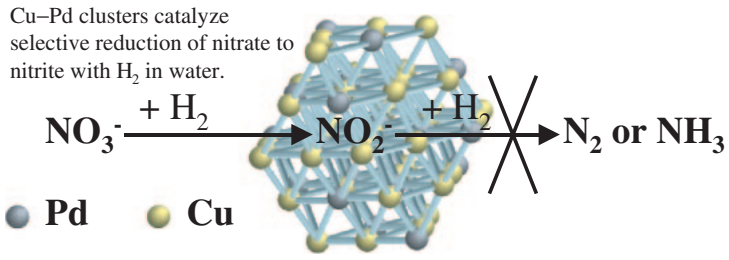

910 **Effect of Lignin on Acetic Acid Production in Wet Oxidation of Lignocellulosic Wastes**

Fangming Jin, Jianxun Cao, Zhouyu Zhou, Takehiko Moriya, and Heiji Enomoto

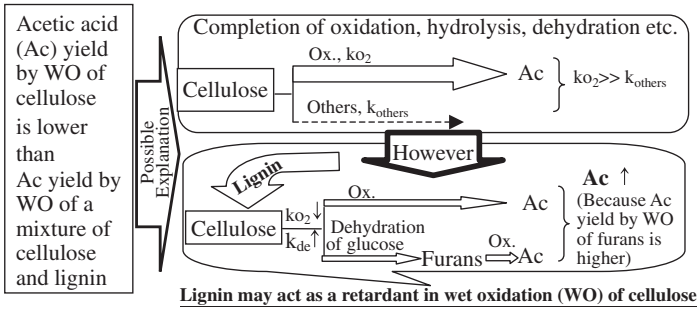

912 **Thermo-responsive Manipulation of a Water Plug in a Poly(*N*-isopropylamide)-modified Glass Capillary**

Tohru Saitoh, Ayahito Sekino, and Masataka Hiraide

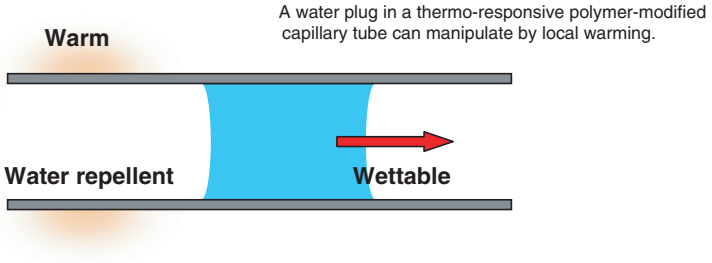

914 **Supramolecular Assembly of [60] Fullerene and Highly Ordered Zinc Octaethylporphyrin Adlayer Formed on Au(111) Surface**

Soichiro Yoshimoto, Eishi Tsutsumi, Yosuke Honda, Osamu Ito, and Kingo Itaya

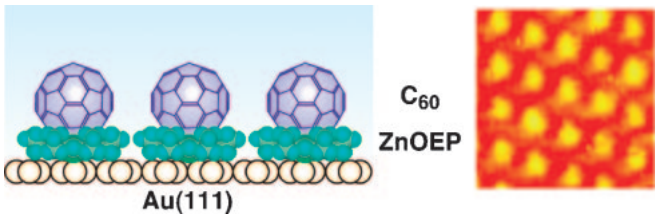

916 **Side Chain Bromination of Mono and Dimethyl Heteroaromatic and Aromatic Compounds by Solid Phase *N*-Bromosuccinimide Reaction without Radical Initiator under Microwave**

Shyamaprosad Goswami, Swapan Dey, Subrata Jana, and Avijit Kumar Adak

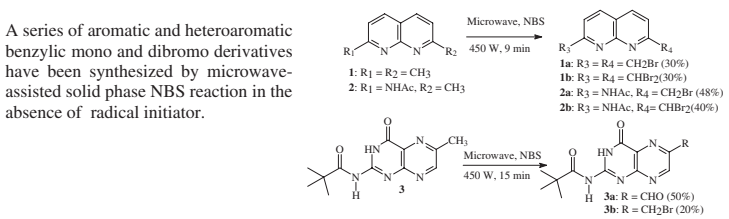

928 **First Transition Metal Complex of 1,8-Bis-(dimethylamino)naphthalene (*proton sponge*)**

First transition metal complexes of 1,8-bis(dimethylamino)naphthalene (*protone sponge*) were synthesized.

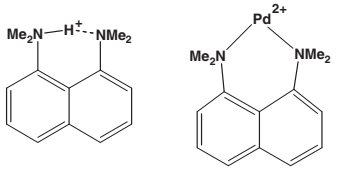

Tomoki Yamasaki, Nobutaka Ozaki, Yasunari Saika, Kozo Ohta, Kenji Goboh, Fumiko Nakamura, Masato Hashimoto, and Seichi Okeya

930 **A Novel Approach for the Preparation of Silver–silica Nanocomposite**

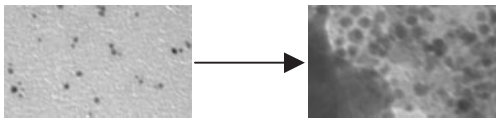

Atanu Mitra and Toyoko Imae

932 **Characterization of the Chiral Paramagnetic Multispin System Built on a Cyclotriphosphazene Scaffold**

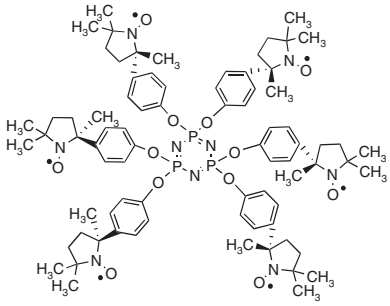

Satoshi Shimono, Rui Tamura, Naohiko Ikuma, Hiroki Takahashi, Naoko Sakai, and Jun Yamauchi

934 **Valence Electron Rules for Three- and Four-membered Atomic Rings: High-row Representative Elements**

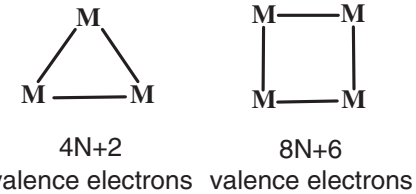

Yi-hong Ding, Kunihiro Takeuchi, and Satoshi Inagaki

936 **Lithium Acetate-catalyzed Mannich-type Reaction between Trimethylsilyl Enolates and Aldimines in a Water-containing DMF**

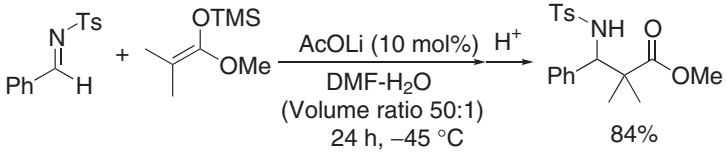

Eiki Takahashi, Hidehiko Fujisawa, and Teruaki Mukaiyama

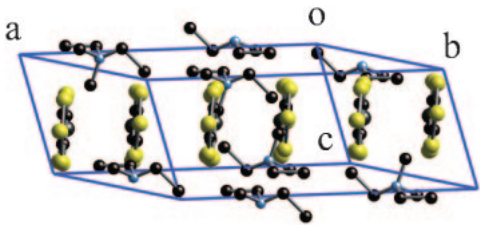

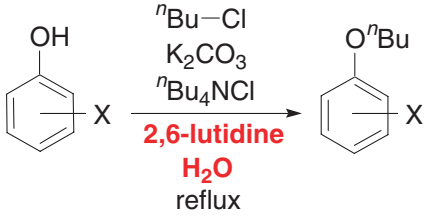

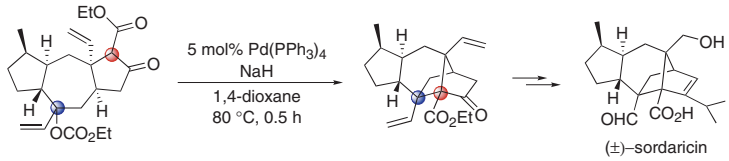

Graphical Abstract for CL-040025 appeared on page C-56 (Vol.33, No.4) should be changed as follows.

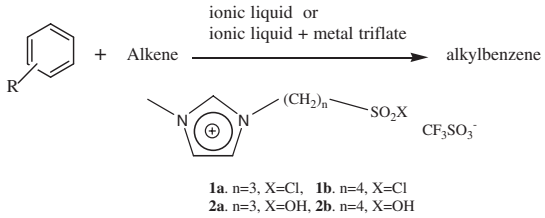

1a. n=3, X=Cl, **1b**. n=4, X=Cl
2a. n=3, X=OH, **2b**. n=4, X=OH

